SSVDAGs: Symmetry-aware Sparse Voxel DAGs

Alberto Jaspe Villanueva
CRS4

Fabio Marton
CRS4

Enrico Gobbetti
CRS4*

Figure 1: *The PowerPlant scene voxelized to a $64K^3$ resolution and stored as a Symmetry-aware Sparse Voxel DAG (SSVDAG). The total non-empty voxel count is nearly 6 billions, stored in less than 86MB at 0.123 bits/voxel. A sparse voxel octree would require 16.2GB without counting pointers, i.e. over 200 times more, while a Sparse Voxel DAG would require 167MB, i.e., nearly the double. Primary rays as well as hard shadow are raytraced directly in the SSVDAG structure, and shading normals are estimated in screen space.*

Abstract

Voxelized representations of complex 3D scenes are widely used nowadays to accelerate visibility queries in many GPU rendering techniques. Since GPU memory is limited, it is important that these data structures can be kept within a strict memory budget. Recently, directed acyclic graphs (DAGs) have been successfully introduced to compress sparse voxel octrees (SVOs), but they are limited to sharing identical regions of space. In this paper, we show that a more efficient lossless compression of geometry can be achieved, while keeping the same visibility-query performance, by merging subtrees that are identical through a similarity transform, and by exploiting the skewed distribution of references to shared nodes to store child pointers using a variabile bit-rate encoding. We also describe how, by selecting plane reflections along the main grid directions as symmetry transforms, we can construct highly compressed GPU-friendly structures using a fully out-of-core method. Our results demonstrate that state-of-the-art compression and real-time tracing performance can be achieved on high-resolution voxelized representations of real-world scenes of very different characteristics, including large CAD models, 3D scans, and typical gaming models, leading, for instance, to real-time GPU in-core visualization with shading and shadows of the full Boeing 777 at sub-millimetric precision.

Keywords: sparse voxel octree, sparse voxel DAG, compression, raycasting, GPU, massive models

Concepts: •**Computing methodologies** → **Ray tracing;** •**Information systems** → *Data compression;*

*CRS4 Visual Computing, POLARIS Ed. 1, 09010 Pula, Italy
www: http://www.crs4.it/vic/
e-mail: {ajaspe|marton|gobbetti}@crs4.it

I3D '16,, February 27–28, Redmond, WA, USA
ISBN: 978-1-4503-4043-4/16/03
DOI: http://dx.doi.org/10.1145/2856400.2856420

1 Introduction

With the increase in performance and programmability of graphical processing units (GPUs), GPU raycasting is emerging as an efficient solution for many real-time rendering problems. In order to handle large detailed scenes, devising compact and efficient scene representation for accelerating ray-geometry intersection queries becomes paramount, and many solutions have been proposed (see Sec. 2). Among these, sparse voxel octrees (SVO) [Laine and Karras 2011] have provided impressive results, since they can be created from a variety of scene representation, they efficiently carve out empty space, with benefits on ray tracing performance and memory needs, and they implicitly provide a levels-of-detail (LOD) mechanism. Given their still relatively high memory cost, and the associated high memory bandwidth required, these voxelized approaches have, however, been limited to moderate scene sizes and resolutions, or to effects that do not require precise geometric details (e.g., soft shadows). While many extremely compact representations for high-resolution volumetric models have been proposed, especially in the area of volume rendering [Balsa Rodriguez et al. 2014], the vast increase in compression rates of these solutions is balanced by increased decompression and traversal costs, which makes them hardly usable in general settings. This has triggered a search for simpler scene representations that can provide compact representations within reasonable memory footprints, while not requiring decompression overhead. Kämpe et al. [2013] have recently shown that, for typical video-gaming scenes, a binary voxel grid can be represented orders of magnitude more efficiently than using a SVO by simply merging together identical subtrees, generalizing the sparse voxel tree to a directed acyclic graph (SVDAG). Such a representation is compact, as nodes are allowed to share pointers to identical subtrees, and remains as fast as SVOs and simple octrees, since the tracing routine is essentially unchanged.

Our approach In this work, we show that efficient lossless compression of geometry can be combined with good tracing performance by merging subtrees that are identical up to a similarity transform, using different granularity at inner and leaf nodes, and compacting node pointers according to their occurrence frequency. The resulting structure, dubbed *Symmetry-aware Sparse Voxel DAG* (SSVDAG) can be efficiently constructed by a bottom-up external-memory algorithm that reduces an SVO to a minimal SSVDAG by alternating different phases at each level. First, all nodes that represent similar subtrees are clustered and replaced by a single representative. Then, pointers to those nodes in the immediately higher level are replaced by tagged pointers to the single representative,

where the tag encodes the transformation that needs to be applied to recover the original subtree from the representative. Finally, representatives are sorted by their reference count, which allows for an efficient variable-bit-rate encoding of pointers. We show that, by selecting planar reflections along the main grid directions as symmetry transform, good building and tracing performance can be achieved.

Contribution Our main contributions are:

- A compact representation of a Symmetry-aware Sparse Voxel DAG that can losslessly represent a voxelized geometry of many real-world scenes within a small footprint and can be efficiently traced;
- An out-of-core algorithm to construct such representation from a SVO or a SVDAG;
- A clean modification of standard GPU raycasting algorithm to traverse and render this representation with small overhead.

Advantages and limitations Our reduction technique is based on the assumption that the original scene representations is geometrically redundant, in the sense that it contains a large amount of subtrees which are similar with respect to a reflective transformation. Our results, see Sec. 6, demonstrate that this assumption is valid for real-world scenes of very different characteristics, ranging from large CAD models, to 3D scans, to typical gaming models. This makes it possible to represent very large scenes at high resolution on GPUs, and to support precise geometric rendering and high-frequency phenomena, such as sharp shadows, with a tracing overhead of less than 15%. Similarly to other works on DAG compression [Kämpe et al. 2013; Sintorn et al. 2014; Kämpe et al. 2015], we focus in this paper only on geometry, and not on non-geometric properties of voxels (e.g., material or reflectance properties), which should be handled by other means.

2 Related Work

Describing geometry for particular applications and devising compressed representation of volumetric models are broad research fields. Providing a full overview of these areas is beyond the scope of this paper. We concentrate here on methods that employ binary voxel grids to represent geometry to accelerate queries in GPU algorithms We refer the reader to a recent survey [Balsa Rodriguez et al. 2014] for a more general overview in GPU-friendly compressed representations for volumetric data.

Starting from more general bricked representations proved successful for semitransparent GPU raycasting [Gobbetti et al. 2008; Crassin et al. 2009], Laine and Karras [2011] have introduced Efficient Sparse Voxel Octrees (ESVOs) for raytracing primary visibility. In their work, in addition to employing the octree hierarchical structure to carve out empty space, they prune entire subtrees if they determine that they are well represented by a planar proxy called contour. Storing the proxy instead of subtrees achieves considerable compression only in scenes with many planar faces, and introduces stitching problems as in other discontinuous piecewise-planar approximations [Agus et al. 2010]. Crassin et al. [2011] have shown the interest of such approaches for secondary rays, computing ambient occlusion and indirect lighting by cone tracing in a sparse voxel octree. Their bricked structure, however, requires large amounts of memory, also due to data duplication at brick boundaries.

A number of works have thus concentrated on trying to reduce memory consumption of such voxelized structures while maintaining a high tracing performance. Crassin et al. [Crassin et al. 2009] mentioned the possibility of instancing, but rely on ad-hoc authoring for fractal scenes, rather than algorithmic conversions. Compression methods based on merging common subtrees have been originally employed in 2D for the lossless compression of binary cartographic images [Webber and Dillencourt 1989], and extended to 3D by Parker and Udeshi [2003] to compress voxel data. These algorithms, however, are costly and require fully incore representations of voxel grids. Moreover, since voxel content is not separated from voxel attributes, only moderate compression is achieved.

High Resolution Sparse Voxel DAGs (SVDAG) [Kämpe et al. 2013] generalize the trees used in Sparse Voxel Octrees (SVOs) to DAGs, allowing the sharing of common octrees. They can be constructed using an efficient bottom-up algorithm that reduces an SVO to a minimal SVDAG, which achieves significantly reduced node count even in seemingly irregular scenes. The effectiveness of the method is demonstrated by ray-tracing high-quality secondary-ray effects using GPU raycasting from GPU-resident SVDAGs. This approach has later been extended to shadowing by voxelizing shadow volumes instead of object geometry [Sintorn et al. 2014; Kämpe et al. 2015]. We improve over SVDAGs by merging subtrees that are identical up to a similarity transform, and present an efficient encoding and building algorithm, with an implementation using reflective transformations. The idea of using self-similarity for compression has also found application in point cloud compression [Hubo et al. 2008], where, however, the focus was on generating approximate representations instead of lossless ones.

In addition to reducing the number of nodes, compression can be achieved by reducing node size. As pointers are very costly in hierarchical structures, a number of proposals have thus focused on reducing their overhead. While pointerless structures based on exploiting predefined node orderings have been proposed for offline storage [Schnabel and Klein 2006], they do not support efficient runtime traversal. The optimizations used for trees, such as grouping children in pages and using relative indexing withing pages [Laine and Karras 2011; Lefebvre and Hoppe 2007] are not applicable to our DAGs, since children are scattered throughout the structure due to sharing. By taking advantage of the fact that the reference count distribution of shared nodes is highly skewed, we thus employ a simple variable bit-rate encoding of pointers.

3 Overview

A 3D binary volumetric scene is a discretized space subdivided in N^3 cells called voxels, which can be empty or full. Since this structure grows cubically for every subdivision, is is hard to achieve high resolutions. SVOs compactify these representation using a hierarchical octree structures of nodes arranged in a number of levels (L), with $N = 2^L$, and most commonly represented using a children bitmask per node as well as up to eight pointers to nodes in the next level. When one of those children represents an empty area, no more nodes are stored under it, introducing sparsity and thus efficiently encoding whole empty areas of the scenes. The structure can be efficiently traversed on the GPU using stackless or short-stack algorithms [Laine and Karras 2011; Beyer et al. 2015], which exploit sparsity for efficient empty-space skipping.

SVOs and grids can be directly created from a surface representation of the scene through a *voxelization* process, for which many optimized solutions have been presented (see, e.g., [Crassin and Green 2012]). In this paper, we use a straightforward CPU algorithm that builds SVOs using a streaming pass over a triangle soup, inserting triangles in an adaptive octree maintained out-of-core using memory-mapped arrays. Using other more optimized solutions would be straightforward.

SVDAGs optimize SVOs by transforming the tree to a DAG, using an efficient bottom-up process that iteratively merges identical nodes

one level at a time and then updates the pointers of the level above. The resulting structure is more compact than SVOs, and can be traversed using the exact same ray-casting algorithm, since node sharing is transparent to the traversal code.

The aim of this work is to obtain a more compact representation of the volume, while keeping the efficiency in traversal and rendering. We do this by merging self-similar subtrees (starting from an SVDAG or an SVO), and by reducing node size through an adaptive encoding of children references.

Among the many possible similarity transformations, we have selected to look for *reflective symmetries*, i.e. mirror transformations along the main grid planes. We thus consider two subtrees similar (and therefore merge them) if their content is identical when transformed by any combination of reflections along the principal planes passing through the node center. Such a transformation $T_{x,y,z}$ has the advantage that the 8 possible reflections can be encoded using only 3 bits (reflection X,Y,Z), that the transformation ordering is not important, as transformations along one axis are independent from the others, and that efficient access to reflected subtrees, which requires application of the direct transformation $T_{x,y,z}$ or of its inverse $T^{-1}_{x,y,z} = T_{x,y,z}$, can be achieved by simple coordinate (or index) reflection. This leads to efficient construction (see Sec. 4.1) and traversal (see Sec. 5). In addition, since the transformation has a geometric meaning, the expectation, verified in practice, is to frequently find mirrored content in real-world scenes (see a 2D example in Fig. 2). The output of the merging process is a DAG in which non-empty nodes are referenced by tagged pointers that encode the transformation $T_{x,y,z}$ that needs to be applied together with the child index. Further compression is achieved by taking advantage of the observation that not all subtrees are uniformly shared, i.e., some subtrees are significantly referenced more than others. We thus use a variable bit-rate encoding, in which the most commonly shared subtrees are references with small indexes, while less common subtrees are referenced with more bits. This is achieved through a per-level node reordering process, followed by a replacement of child pointers by indices. The encoding process, as well as the resulting final encoding is described in Sec. 4.2.

4 Construction and encoding

A SSVDAG is constructed bottom-up starting from a voxelized representation (SVDAG or SVO). We first explain how a minimal SSVDAG is constructed by merging similar subtrees, and then explain how the resulting representation is compactly encoded in a GPU-friendly structure.

4.1 Bottom-up construction process

Constructing the SSVDAG requires to efficiently find reflectively-similar subtrees. Since explicitly checking similarity in subtrees would be prohibitively costly for large datasets, we use a bottom-up process that iteratively merges similar nodes one level at a time. This requires, however, some important modifications to the original SVDAG construction method. In our technique, we start from an out-of-core structure, maintained in memory-mapped external-memory arrays that encodes, level-by-level the existing nodes using one array per level. We start the construction process from the finest level $L-1$, and proceed up to the root at level 0.

Our construction code is capable to perform a transformation into a DAG with or without symmetries, and works, for compatibility with previous encoding methods, using a leaf size of 2^3. Grouping into larger leaves is performed in post-processing during our encoding phase (see Sec. 4.2). At each level, we first group the nodes into cluster of self-similar nodes, then select one single representative per cluster and associate to others the transformation that maps them to the representative. The surviving nodes are reordered for compact encoding (see Sec. 4.2) and stored in the final format. Child pointers of nodes at the previous level are then updated to point to the representatives, and the process is repeated for all levels up to the root.

The matching process at the core of clustering is based on the concept of reordering the nodes at a given level so that matching candidates are stored nearby. Clustering and representative selection is then performed during a streaming pass. Leaf nodes and inner nodes, must use, however, different methods to compute ordering and perform matching.

Leaf nodes clustering In order to efficiently match leaf nodes in the tree, we must discover which representation of small voxel grids remain the same when one of the possible transformations is applied. Considering that each grid G can be represented by a binary number $B(G)$ by concatenating all the voxel occupancy bits in linear order, we define a mapping of each possible grid G to another grid $G^\star = T^\star_{x,y,z}(G)$, such that the *canonical transformation* $T^\star_{x,y,z} = \arg\max_{T_{x,y,z}} B(T_{x,y,z}(G))$. $G^\star$ is the *canonical representation* of G, and represents, among all possible reflections of G, the one with the largest integer value. Geometrically, it is the one that attracts most of the empty space to the origin (see Fig. 3). This transformation is precomputed in a table of 256 entries that maps all the possible combinations of 2^3 voxels to the bitcode representing the canonical transformation as well as to the unique canonical representation (one of the 46 possible ones). Given this transformation, two nodes are self-similar if their canonical representation is the same. Clustering can thus be performed in a single streaming pass after sorting leaves using the canonical representation as a key. Nearby nodes sharing the same canonical representation are merged into a single representative, pointers at the upper level are then updated to point to the representative, and pointer tags are computed so as to obtain the original leaf from the representative.

Inner nodes clustering While for leaf nodes we can detect symmetries by directly looking at their bit representation, two inner nodes n_1 and n_2 must be merged if they represent the exact same *subtrees* when a transformation T is applied. The first trivial condition to be checked is that child pointers must be the same. We thus sort the inner nodes using the lexicographically sorted set of pointers to children as key. Since after sorting all self-similar nodes are positioned nearby, as they are among those that share the same set of pointers, we perform merging by creating, during a streaming pass, one representative per group of self-similar nodes. The self-similarity condition must be verified without performing a full subtree comparison. Given the properties of our reflective transformations, we have thus to verify that, when the two nodes n_1 and n_2 are matched for similarity under a candidate transformation T, every tagged pointer (tag, p) of n_1 is mapped to $(T(tag), p)$ in n_2 if p is not invariant to the transformation T, or it is mapped to $(T(tag) \bigvee \neg T(tag), p)$ if it is invariant (see Fig. 4). This means, for instance, that, when looking for a match under a left-right transformation T_x, the left and right pointers must be swapped in n_2 with respect to n_1, and the pointed subtrees must be equal under a left-right mirroring, The latter condition is verified if the pointed subtree has a left-right symmetry, or if, for each matched pair of tagged child pointers, the left-right transformation bit is inverted while the other bits are the same. This process does the clustering for one particular transformation T, and is repeated for each of the 8 possible reflection combinations, stopping at the first transformation that generates a match with one of the currently selected representatives, or creating a new representative if all tests are unsuccessful. In order to efficiently implement invariance checks, we thus asso-

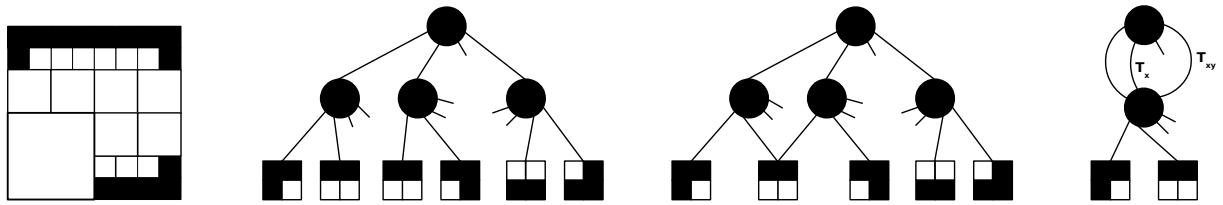

Figure 2: *Example 2D scene transformed into different structures. The Sparse Voxel Octree (SVO) contains 10 nodes. The Sparse Voxel Directed Acyclic Graph (SVDAG) finds one match and then shares a node, meaning 9 nodes. The presented Symmetry-aware Sparse Voxel Directed Acyclic Graph (SSVDAG) finds reflective matches in two last levels, and reduces the structure to 4 nodes.*

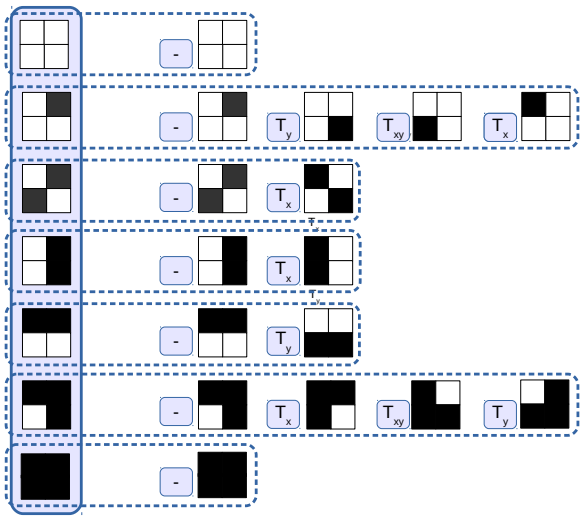

Figure 3: *2D example of canonical transformations of a small voxel grid into a set of base representatives. The transformation maps clusters of self-similar grids to a unique representative.*

ciate three invariant bits (one for each mirroring direction) at each of the leaves when computing their canonical representations, and pull them up during construction at inner nodes by suitably combining the invariant bits of pointed nodes at each merging step. For instance, an inner node is considered invariant with respect to a left-right transformation if all its children are invariant with respect to that transformation, or the left children are the mirror of the right ones.

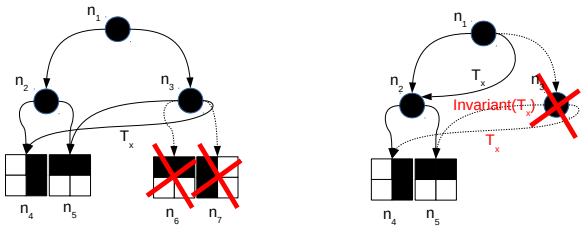

Figure 4: *On the left, during leaf clustering, references to leaf node n_6 are replaced by references to n_5, which is identical, while references to n_7 are replaced with references to n_4 transformed by transformation T_x. On the right, inner node n_3 is replaced with n_2 through transformation T_x since its left child n_5 is invariant to transformation T_x and is identical to the right child of n_2, while its right child matches the left child of n_2 through the same transformation T_x.*

4.2 Compact encoding

The outlined construction process produces a DAG where inner nodes point to children through tagged pointers that reference a child and encode the transformation that has to be applied to recover the original subtree. We encode such a structure in a GPU friendly format aimed at reducing the pointer overhead, while supporting fast tracing without decompression. We achieve this goal through leaf grouping, frequency-based pointers compaction, and memory-aligned encoding.

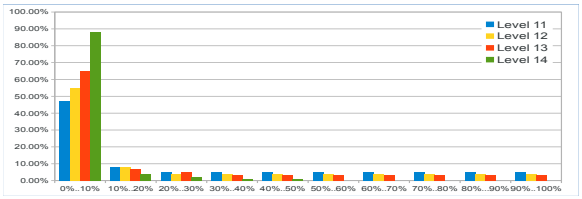

Figure 5: *Histograms of the references to nodes in the Powerplant dataset voxelized at $64K^3$ resolution, with nodes sorted by reference counts. As we can see, the distribution is highly skewed, and the most popular 10% of the nodes account for most of the references.*

Leaf grouping While 2^3 allow for an elegant construction method using table-based clustering, such a level of granularity leads to a high structure overhead, since rays have to traverse deep pointer structures to reach small 8-voxel grids, and the advantage of clustering is offset by the need to encode pointers to these small nodes. For final encoding, we have thus decided to coarsen the construction graph by one level, encoding as simple grids all the 4^3 grids, and to store them in a single array of bricks, each occupying 64 bits. Note that this decision does not require performing new matches on 4^3 leaves, since we just coarsen the graph obtained with the bottom-up process described in Sec. 4.1, which uses a table-based matching on 2^3 leaves at level $L-1$ to drive the construction of 4^3 inner nodes at level $L-2$.

Frequency-based pointer compaction We have verified that in our SSVDAG the distributions of references to nodes is highly skewed. This means that there typically is a small groups of node referenced by a lot of parents nodes, while many others are referenced much less. Fig. 5, for instance, shows the histogram of the distribution of reference counts in the Powerplant dataset of Fig. 1, where the most common 10% of the nodes is referenced by nearly 90% of pointers at level 14 (nearly 50% at level 11). We have thus adopted an approach in which frequently used pointers are represented with less bits than more frequent ones. In order to do that, for encoding, we reorder nodes at each level using the number of references to it as a key, so that most referenced nodes appear first in a level's array. We then replace pointers with offsets from the beginning of each level array, and chose for each offset the smallest number of bits available in our encoded format (see below).

Memory aligned encoding While leaf nodes are all of the same size (64 bits), the resulting inner node encoding produces variable-sized records (which is true also for other DAG formats with variable child count, e.g., SVDAG [Kämpe et al. 2013]). We have decided, in order to simplify decoding, to use half-words (16 bits) as the basis for our encoding. Our final encoding includes an indexing structure, an array of inner nodes, and an array of leaf nodes. The indexing structure contains the maximum level L and three 32-bits offsets in the inner level array that indicate the start of each level. The layout of inner-level nodes is depicted in Fig. 6. For each node, we store in a 16-bit header a 2-bit code for each of the 8 potential children. Tag 00 is reserved to null pointers, which are not stored, while the other tags indicate the format in which child pointers are stored after the header. Children of type 01 use 16 bits, with the leftmost 3 bits encoding the transformation, while the remaining 13 bits encode the offset in number of level-words from the beginning of the next level, where a level-word is 2 bytes for an inner level and 8 bytes for the leaf level. Thus, reflections and references to nodes stored in the first 2^{14} bytes of an inner level's array or in the first 2^{16} bytes of the leaf level can be encoded with just two bytes. Less frequent children pointers, associated to header tags 10 and 11, are both encoded using 32 bits, with the leftmost 3 bits encoding the transformation, and the rightmost ones the lowest $29bits$ of the offset. The highest bit of the offset is set to the rightmost bit of the header tag. We can thus address more than $2GB$ into an inner level, and $8GB$ into leaves.

Figure 6: *Layout of inner nodes in our compact representation.*

5 Ray-tracing a SSVDAG

The SSVDAG structure can be efficiently traversed using a GPU-based raytracer by slightly adapting other octree-based approaches to apply the transformation upon entering a subtree.

In order to test several approaches within the same code base, we have implemented a basic GPU-based raytracer in GLSL to traverse both SVO, SVDAG, and our SSVDAG. While the structure alone, similar to SVDAG [Kämpe et al. 2013], is mostly useful for visibility queries and/or secondary rays effects, in order to fully test the structure in the simplest possible setting, we use the raytracer both from primary rays (requiring closest intersections) and for hard shadows for the view samples of a deferred rendering target. We focus on these effects, rather than soft shadows and ambient occlusion, since they are the ones where voxelization artifacts are most evident. The normals required for shading are obtained by finite differences in the frame buffer using a discontinuity preserving filter. While in other settings other structures can be used for storing normals and material properties (see, e.g., [Kämpe et al. 2013]), this approach also shows a practical way to implement real-time navigation of very large scenes from a compressed representation.

Our dataset is fully stored in two texture buffer objects, one for the inner nodes, and one for the leaves. For large datasets that exceed texture buffer objects addressing limits, we use 3D textures. Similarly to previous work [Laine and Karras 2011; Kämpe et al. 2013], raycasting traverses the voxels intersected by the ray using a depth-first visit of the octree based on a recursive digital differential analyzer implemented using a full stack. Traversal stops when a non-empty voxel is found or the ray span is terminated. The only algorithmic modification to the regular approach occurs when the algorithm needs follow child pointers, since children are stored in our compact format using a variable-rate encoding, and every time we enter a child we we must apply the transformation stored with the pointer referencing it.

As in SVDAG [Kämpe et al. 2013], we must access the i-th children pointer by computing an offset within the header equal to the size of all pointers in the interval $[0, i-1]$, with the only difference that in SVDAG the only two size possibilities are 0 and 4, while in our case tagged pointers can be stored using 0, 2, and 4 bytes. This computation is performed in our shader using a manually unrolled loop.

Once the tagged pointer to the child is found, the associated transformation code is given by the 3 highest bits, and should be applied to all the nodes in the subtree. We therefore maintain during traversal a 3-bit transformation status, which indicates whether which reflections must be applied to the indices used to access child pointers in inner nodes or voxel contents in lead nodes. The transformation status is initialized at 0, is updated each time we descend in a child by xor-ing it with the pointer's reflection tag, and is pushed to the stack together with the current node to be able to restore it upon backtracking.

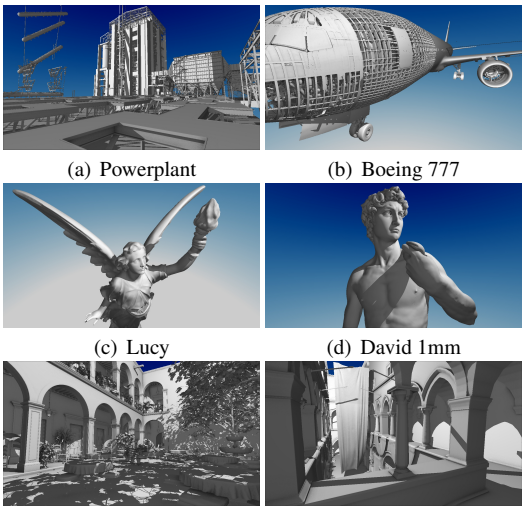

(a) Powerplant (b) Boeing 777

(c) Lucy (d) David 1mm

(e) San Miguel (f) Crytek Sponza

Figure 7: *The scenes used in our experiments. All images are interactively rendered using our raytracer from fully GPU-resident data using deferred shading with screen-space normal estimation and hard shadows.*

6 Results

An experimental software library, preprocessor and viewer application have been implemented on Linux using C++, OpenGL and GLSL shading language. All the processing and rendering tests have been performed on a Desktop Linux PC equipped with an Intel Core i7-3820, 64 GB of RAM and an NVIDIA GeForce 980 GTX with 4GB of video memory.

6.1 Datasets

We have extensively tested our system with a variety of high resolution surface models. Here we present six models which have been selected to cover widely different fields: CAD, 3D scans and videogaming (see Fig. 7). The CAD models, the Powerplant (12 MTriangles) and the extremely large and complex Boeing 777 (350M triangles) have been chosen to prove the effectiveness of our method with extremely high resolution datasets with connected interweaving detailed parts of complex topological structure, thin and curved tubular structures, as well as badly tessellated models that do not always create closed volumes. The 3D Scans represent, Lucy (28M triangles) and Michelangelo's David 1mm (56M triangles), are representatives of dense high resolution scans of man-made objects

with small details and smooth surfaces. The fourth and fifth model are the San Miguel dataset (7.8M triangles) and the Crytek Sponza dataset (282K triangles)), which are similar to what can be found on a video-game settings, and, together with Lucy, also provide a direct comparison point with the work on SVDAGs [Kämpe et al. 2013] .

Table 1: *Compression performance reduction from SVDAGs to SSVDAGs. Resolutions are stated in the top row. For each dataset, the first row is the total time, and the second row is the count of non-empty voxels.*

Dataset		$2K^3$	$4K^3$	$8K^3$	$16K^3$	$32K^3$	$64K^3$
Powerplant	Time (s)	0.2	0.6	1.5	3.8	10.1	28.1
	MVox	4	17	72	310	1336	5827
Boeing 777	Time s	1.2	5.0	23.2	86.3	356.0	1517.1
	MVox	12	57	268	1242	5699	24633
Lucy	Time s	0.5	1.8	7.5	31.4	121.5	399.1
	MVox	6	25	99	395	1580	6321
David 1mm	Time s	0.4	1.3	4.9	21.6	83.1	290.0
	MVox	4	16	64	257	1029	4116
San Miguel	Time s	0.3	1.2	4.4	15.9	52.7	176.7
	MVox	12	46	187	750	3007	12045
Crytek Sponza	Time s	0.5	1.6	4.7	15.1	45.5	124.7
	MVox	40	160	641	2568	10276	41124

6.2 DAG reduction speed

The preprocessor transforms a 3D triangulation into a SVO stored on disk and then compresses it using different strategies. Preprocessing statistics for the various datasets at different resolutions are reported in Table 1. For brevity, we report here timings relative to the conversion from a SVDAG to SSVDAG. which corresponds to the part related to node reduction by self-similarity and frequency-based pointer encoding. As a comparison, Crassin et al. [2012] report for the Crytek Sponza dataset a building time of 7.34ms for the resolution 512^3 on an NVIDIA GTX680 GPU, and Kämpe et al. [Kämpe et al. 2013] report 4.5s for building an SVDAG from a SVO at resolution $8K^3$ on an Intel Core i7-3930, i.e., similar to our conversion from SVDAG to SSVDAG. Note that these approaches assume that the the intermediate SVO, and the final DAG need to fit into memory, while we implement an out-of-core approach. Recently, Pätzold and Kolb [Pätzold and Kolb 2015] have presented a scalable voxelization approach that builds SVOs from triangle soups using external memory. Their code builds a $8K^3$ SVO for the Crytek Sponza dataset in 98s. Our conversion times are thus similar to previous node reduction works, and are in any case about an order of magnitude faster than the first step required for creating an SVO from the original dataset. About 4% of the time in our conversion is due to the frequency-based pointer compaction step, which requires a reordering of nodes performed in external memory.

6.3 Compression performance

Table 2 provides detailed information on processing statistics and compression rates of all the test models. We compare our compression results to SVDAG [Kämpe et al. 2013], as well as to the pointerless SVOs [Schnabel and Klein 2006], where each node consumes one byte, a structure that cannot be traversed in random order but useful for off-line storage. For a comparison with ESVO [Laine and Karras 2011], please refer to the original paper on SVDAGs [Kämpe et al. 2013]. It should be noted that the slight differences in number of non-empty nodes in the SVO structure with respect to Kämpe et al. [2013] is due to the different voxelizers used in the conversion from triangle meshes.

Memory consumption obviously depends both on node size and node count. We therefore include for our structure results using uncompressed nodes (USSVDAG in Table 2), with the same encoding employed for SVDAGs [Kämpe et al. 2013], as well as results using our optimized layout (SSVDAG in Table 2). SVDAGs cost 8 to 36 bytes per node, depending on the number of child pointers. Our uncompressed SSVDAGs have the same cost, since symmetry bits are stored in place of padding bytes. On the other hand, our compressed SSVDAGs cost 4 to 34 bytes per node, depending both on the number of child pointers and their size, computed according on the basis of a frequency distribution. In order to assess the relative performance of our different optimizations, we also include results obtained without including symmetry detection but encoding data using our compact representations (ESVDAG).

As we can see, all the DAG techniques outperform the pointerless SVO consistently at all but the lower resolutions, even though they offer in addition full traversal capabilities. Moreover, our strategies for node count and node size reduction prove successful. The USSVDAG structure, on average, occupies at $64K^3$ resolution only 79.6% of the storage required by the SVDAG structure, thanks to the equivalent reduction in the number of nodes provided by our similarity matching strategy. An average reduction in size to about 52.4% of the SVDAG encoding is obtained by also applying the frequency-based tagged pointer compaction strategy. Such a strategy is particularly successful since, by matching more pointers, increased opportunities for referencing highly popular nodes arise. This is also proved by the results obtained by the ESVDAG techniques, which uses our data structure but only matches sub-trees if they are equal, as in the original SVDAG. The stronger compression of SSVDAGs makes it possible, for instance, to easily fit all the Boeing model into a 4GB graphics board (GeForce GTX 980) at $64K^3$ resolution. Since the Boeing 777 airplane has a length of 63.7m and a wingspan of 60.9m, using a $64K^3$ grid permits to represent details with sub-millimetric accuracy (see Fig. 8).

6.4 Rendering

Since our main contributions target compression, we have not optimized our raytracing implementation, focusing on verifying correctness of construction and relative performance of the methods rather than absolute speed. We have thus implemented a generic shader-based raytracer that shares general traversal code based for the various DAG structures. The different structures are supported by simply specializing the general code through structure-specific versions of the routines that read a node structure, access a child by following a pointer, and applies transformation to a ray (see Sec. 5 for details), The SVDAG and USSVDAG version access nodes by fetching data from a GL_R32UI texture buffer object, while SSVDAG uses a GL_R16UI buffer because of the different alignment requirements. 3D textures are used in place of texture buffer objects when the data is so large to exceed buffer addressing limits. This happens only for the Boeing at $64K^3$ resolution for the results presented in this paper. The code does not use any other acceleration or shading structure, and normals required for shading are generated in screen space. This simple setup also shows that it is possible to use such a terse structure to support interactive navigation of very large models compressed to the GPU.

As illustrated in our accompanying video, we have obtained similar relative performances for all the models. For instance, for the three sample viewpoints in Fig. 1 of the Powerplant model at $64K^3$ resolution, the overall view on the left is rendered at 74fps with SSVDAG, 86fps with USSVDAG, and 87fps with SVDAG. The results for the center image are, instead of 70fps for SSVDAG, 81fps for USSVDAG, and 82fps for SVDAG. Finally, the results for the right closeup image are, instead, of 36fps for SSVDAG, 42fps for USSVDAG, 43fps for SVDAG. All images are rendered in HD (720p) with screen-space normal estimation and hard shadows for one point light. Rendering performance is thus similar for the three implementations. demonstrating that the reduction in memory con-

Table 2: *Comparison of compression performance for various data structures: our Symmetry-aware Sparse Voxel DAG (SSVDAG) is compared with the original sparse voxel DAG (SVDAG), and the pointerless SVO. In order to evaluate the effects of the different optimizations, we also provide results for a version of SSVDAG without pointer compression (USSVDAG) and without symmetry detection (ESVDAG). Resolutions are stated in the top row. On the left, we show the total node count at 2^3 resolution. On the right, we show the total memory consumption of the resulting dataset. The last column states memory consumption per non-empty cubical voxel in the highest built resolutions ($64K^3$).*

Scene		Total number of nodes in millions						Memory consumption in MB						bits/vox
		$2K^3$	$4K^3$	$8K^3$	$16K^3$	$32K^3$	$64K^3$	$2K^3$	$4K^3$	$8K^3$	$16K^3$	$32K^3$	$64K^3$	$64K^3$
Powerplant	SSVDAG	0.1	0.2	0.4	1.0	2.3	5.4	0.7	2.0	5.2	13.3	33.8	85.8	0.123
12 MTri	USSVDAG	"	"	"	"	"	"	1.6	4.0	9.7	23.1	54.9	130.5	0.188
	ESVDAG	0.1	0.2	0.5	1.2	2.9	7.0	0.8	2.4	6.3	16.2	41.9	108.6	0.156
	SVDAG	"	"	"	"	"	"	1.9	4.9	11.8	28.7	69.9	167.3	0.241
	SVO	1.1	5.0	22.0	94.4	404.9	1741.0	1.1	4.8	20.9	90.05	386.2	1660.3	2.390
Boeing 777	SSVDAG	0.3	0.9	3.2	11.3	40.0	140.0	3.0	11.7	43.1	162.9	616.2	2314.4	0.788
350 MTri	USSVDAG	"	"	"	"	"	"	6.9	24.8	83.8	295.0	1042.8	3671.5	1.250
	ESVDAG	0.4	1.3	4.3	14.4	48.3	164.4	3.9	15.2	54.0	199.1	731.1	2740.7	0.933
	SVDAG	"	"	"	"	"	"	9.2	33.8	112.9	376.7	1260.6	4307.9	1.467
	SVO	3.3	15.6	72.8	341.0	1582.8	7282.0	3.1	14.9	69.4	325.2	1509.5	6944.6	2.365
Lucy	SSVDAG	0.1	0.4	1.4	4.8	14.4	40.3	1.5	5.3	19.1	67.2	213.6	642.2	0.852
28 MTri	USSVDAG	"	"	"	"	"	"	2.9	9.2	32.3	110.3	332.4	915.5	1.215
	ESVDAG	0.2	0.5	1.7	5.7	18.3	52.9	2.1	6.8	24.0	86.5	295.1	896.5	1.190
	SVDAG	"	"	"	"	"	"	4.0	11.3	36.8	127.3	419.0	1212.0	1.608
	SVO	2.0	8.2	32.9	131.6	526.6	2106.8	2.0	7.8	31.3	125.5	502.2	2009.2	2.666
David 1mm	SSVDAG	0.1	0.3	1.1	3.6	11.2	31.8	1.1	3.9	13.6	48.1	159.2	486.7	0.992
56 MTri	USSVDAG	"	"	"	"	"	"	2.2	7.0	23.3	79.7	252.7	716.1	1.459
	ESVDAG	0.1	0.4	1.3	4.2	13.8	41.5	1.5	5.0	17.1	61.3	214.3	683.3	1.393
	SVDAG	"	"	"	"	"	"	3.0	8.8	27.3	91.8	308.0	938.6	1.913
	SVO	1.3	5.4	21.5	85.9	343.2	1372.4	1.3	5.1	20.5	81.9	327.3	1308.8	2.667
San Miguel	SSVDAG	0.1	0.3	0.9	2.6	7.7	21.6	1.0	3.3	10.3	31.9	98.7	295.9	0.206
7.8 MTri	USSVDAG	"	"	"	"	"	"	2.1	6.9	21.3	61.8	181.1	509.8	0.355
	ESVDAG	0.1	0.3	1.1	3.1	9.1	26.5	1.1	3.7	12.0	37.6	118.7	373.0	0.260
	SVDAG	"	"	"	"	"	"	2.3	7.8	24.6	72.0	212.2	621.3	0.433
	SVO	3.8	15.3	61.7	248.2	997.8	4004.4	3.6	14.6	58.9	236.7	951.6	3818.9	2.660
Crytek Sponza	SSVDAG	0.1	0.4	1.1	2.9	7.6	19.7	1.7	5.2	15.1	42.1	115.7	315.3	0.064
282 KTri	USSVDAG	"	"	"	"	"	"	3.4	9.7	25.8	67.4	172.3	436.8	0.089
	ESVDAG	0.2	0.5	1.4	3.7	9.8	25.5	2.1	6.4	18.8	53.6	151.3	417.3	0.085
	SVDAG	"	"	"	"	"	"	4.2	11.9	31.8	83.6	218.3	563.5	0.115
	SVO	12.8	52.6	212.6	853.9	3421.5	13697.4	12.21	50.2	202.7	814.3	3263.0	13062.9	2.665

sumption does not come at the cost of much increased render times. It should be noted that reflections impose a very little overhead, since USSVDAG is only 1%-2% slower than SVDAG, while pointer compresssion proves a little bit more costly, since SSVDAG has an overhead of 14%-16% with respect to SVDAG. This is probably due to the fact that, while the extra computation required for implementing reflections is well hidden by memory latency, the more elaborate memory layout of pointer compression is more costly. This aspect leaves room for optimization.

Even with our unoptimized shader-based implementation, our SSVDAG structure supports real-time performance for very complex scenes. The Boeing 777 scene can be explored at $64K^3$ resolution in HD (720p) with shading and shadows, at about the same performance as the Powerplant model. Fig. 8 shows images taken from the same closeup viewpoint rendered with various voxel resolutions. It is evident how the small voxel dimensions enabled by our compression let appreciate important details that are lost at lower resolutions. The highest resolution is only possible with our SSDAG and USSDAG methods, which are the only ones capable to fit the entire model in-core in a 4GB board. We expect major speedups with a more elaborate implementation, e.g., supporting beam optimization.

7 Conclusions and Future Work

We have shown that Symmetry-aware Sparse Voxel DAGs (SSDAGs), an evolution of Sparse Voxel DAGs, allow for an efficient lossless encoding of voxelized geometry representations, in which subtrees that are identical up to a similarity transformations appear only once. Our results demonstrate that this sort of geometric redundancy is common in all tested real-world scenes, ranging from complex CAD models to 3D scans to gaming models, leading to state-of-the-art lossless compression performance. The increased node size with respect to SVOs and SDAGs is quickly balanced by the good reduction in node count. Moreover, pointer overhead is reduced by using fatter leaves and a simple entropy coding. The resulting structure is compact and GPU-friendly, which makes it possible to trace very large scenes while maintaining the visibility acceleration structure fully resident in GPU memory. As the structure can be efficiently constructed from external memory, the resulting method is fully applicable to massive data sets.

Many interesting areas remain for future work. While the current implementation uses reflections only, an interesting avenue for future work would be to investigate other symmetries. Rearranging nodes based on reference frequency has proven useful to reduce pointer overhead. Such rearranging techniques could be further expanded, for example to achieve a better encoding in low-sharing areas. While in this work we have focused only on visibility query acceleration, adding a material representation is also of great interest.

Acknowledgments

This work is partially supported by the EU FP7 Program under the DIVA project (REA 290277) and by Sardinian Regional Authorities under the VIGEC and HELIOS projects. Datasets are courtesy of the University of North Carolina at Chapel Hill (Powerplant), Dave Kasik and The Boeing Company (Boeing 777), the Stanford 3D

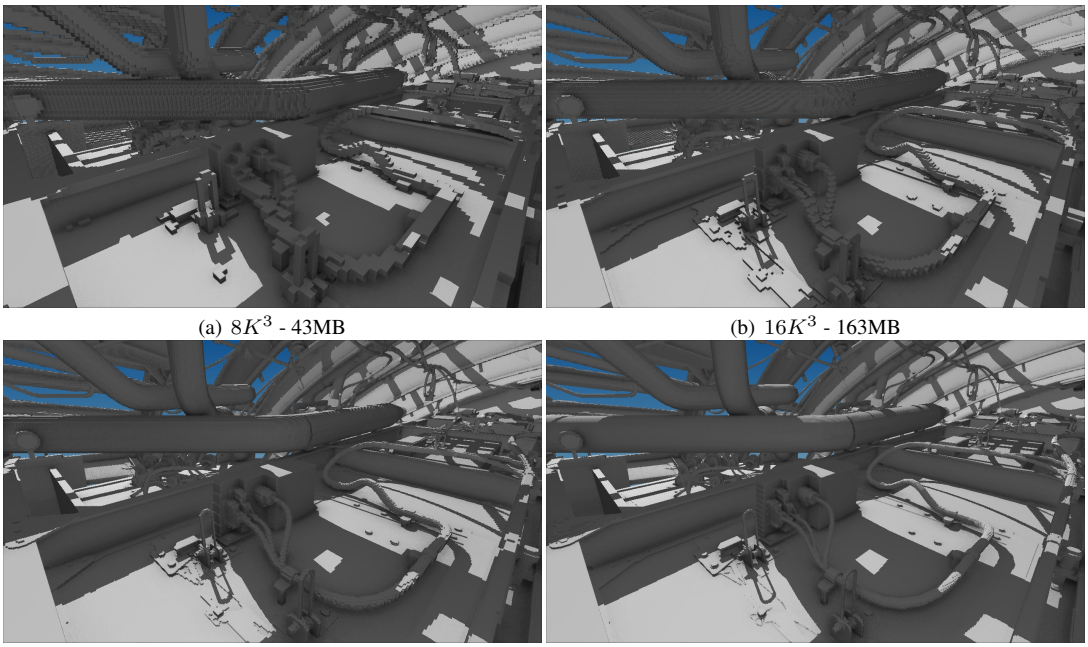

(a) $8K^3$ - 43MB (b) $16K^3$ - 163MB

(c) $32K^3$ - 617MB (d) $64K^3$ - 2331MB

Figure 8: *Detail view of the Boeing scene at different resolutions. The compression performance of our method supports real-time rendering from GPU-resident data even at $64K^3$ resolution, while SVDAG memory requirements exceed on-board memory capacity on a 4GB board (see Table 2).*

Scanning and Digital Michelangelo Repositories (Lucy, David), G. M. Leal Llaguno (San Miguel), and F. Meinl (Crytek Sponza). We thank Ulf Assarsson and Erik Sintorn (Chalmers University) for helpful discussions.

References

AGUS, M., GOBBETTI, E., IGLESIAS GUITIÁN, J. A., AND MARTON, F. 2010. Split-Voxel: A simple discontinuity-preserving voxel representation for volume rendering. In *Proc. Volume Graphics*, 21–28.

BALSA RODRIGUEZ, M., GOBBETTI, E., IGLESIAS GUITIÁN, J., MAKHINYA, M., MARTON, F., PAJAROLA, R., AND SUTER, S. 2014. State-of-the-art in compressed GPU-based direct volume rendering. *Computer Graphics Forum 33*, 6, 77–100.

BEYER, J., HADWIGER, M., AND PFISTER, H. 2015. State-of-the-art in GPU-based large-scale volume visualization. In *Computer Graphics Forum*. In press.

CRASSIN, C., AND GREEN, S. 2012. Octree-based sparse voxelization using the GPU hardware rasterizer. *OpenGL Insights*, 303–318.

CRASSIN, C., NEYRET, F., LEFEBVRE, S., AND EISEMANN, E. 2009. Gigavoxels: Ray-guided streaming for efficient and detailed voxel rendering. In *Proc. ACM I3D*, 15–22.

CRASSIN, C., NEYRET, F., SAINZ, M., GREEN, S., AND EISEMANN, E. 2011. Interactive indirect illumination using voxel cone tracing. In *Computer Graphics Forum*, vol. 30, 1921–1930.

GOBBETTI, E., MARTON, F., AND IGLESIAS GUITIÁN, J. A. 2008. A single-pass GPU ray casting framework for interactive out-of-core rendering of massive volumetric datasets. *The Visual Computer 24*, 7-9, 797–806.

HUBO, E., MERTENS, T., HABER, T., AND BEKAERT, P. 2008. Self-similarity based compression of point set surfaces with application to ray tracing. *Comput. Graph. 32*, 2 (Apr.), 221–234.

KÄMPE, V., SINTORN, E., AND ASSARSSON, U. 2013. High resolution sparse voxel DAGs. *ACM Trans. Graph. 32*, 4, 101:1–101:13.

KÄMPE, V., SINTORN, E., AND ASSARSSON, U. 2015. Fast, memory-efficient construction of voxelized shadows. In *Proc. ACM I3D*, 25–30.

LAINE, S., AND KARRAS, T. 2011. Efficient sparse voxel octrees. *IEEE Trans. Vis. Comput. Graph 17*, 8, 1048–1059.

LEFEBVRE, S., AND HOPPE, H. 2007. Compressed random-access trees for spatially coherent data. In *Proc. EGSR*, 339–349.

PARKER, E., AND UDESHI, T. 2003. Exploiting self-similarity in geometry for voxel based solid modeling. In *Proc. ACM Solid Modeling*, 157–166.

PÄTZOLD, M., AND KOLB, A. 2015. Grid-free out-of-core voxelization to sparse voxel octrees on gpu. In *Proc. High-Performance Graphics*, 95–103.

SCHNABEL, R., AND KLEIN, R. 2006. Octree-based point-cloud compression. In *Proc. SPBG*, 111–120.

SINTORN, E., KÄMPE, V., OLSSON, O., AND ASSARSSON, U. 2014. Compact precomputed voxelized shadows. *ACM Trans. Graph. 33*, 4 (July), 150:1–150:8.

WEBBER, R. E., AND DILLENCOURT, M. B. 1989. Compressing quadtrees via common subtree merging. *Pattern recognition letters 9*, 3, 193–200.